Thin Solid Films 519 (2011) 7476–7480

Contents lists available at ScienceDirect

Thin Solid Films

journal homepage: www.elsevier.com/locate/tsf

Baseline model of graded-absorber Cu(In,Ga)Se_2 solar cells applied to cells with $Zn_{1-x}Mg_xO$ buffer layers

J. Pettersson *, C. Platzer-Björkman, U. Zimmermann, M. Edoff

Ångström Solar Center, Solid State Electronics, Uppsala University, P. O. Box 534, SE-751 21 Uppsala, Sweden

ARTICLE INFO

Available online 23 December 2010

Keywords:
Electrical modelling
CIGS solar cells
Buffer layers
Graded absorber
Light soaking
Metastabilities

ABSTRACT

A baseline parameter set for electrical modelling of Cu(In,Ga)Se_2 solar cells with compositionally graded absorber and CdS buffer layer is established. The cases with and without Fermi level pinning as well as with and without a surface defect layer are considered. Simulations with a defect layer are observed to give the best correspondence to measurements. $Zn_{1-x}Mg_xO$ buffer layers are introduced and initial modelling of the light soaking behaviour is performed. Simulation results are compared with experimental data.

1. Introduction

Solar cell modelling can be a valuable tool for gaining a deeper knowledge into the physical background of phenomena visible in electrical measurements. In this work a baseline set of parameters for electrical modelling of Cu(In,Ga)Se_2 (CIGS) solar cells with CdS buffer layer and absorber layer from our micro pilote line, is introduced. Details about the processing of these cells can be found in Ref. [1–3]. Electrical modelling is performed using the one-dimensional software SCAPS [4]. Current–voltage (JV) and quantum-efficiency (QE) curves are simulated and compared with experimental data. One property of CIGS solar cells which is much debated is if the Fermi level is pinned at the interface between the CIGS and CdS layers or not [5–7]. Both situations are considered here. It has been found experimentally on $CuInSe_2$ films that the surface can be copper poor with a bandgap wider than the bulk [8–11]. The nature of this surface defect layer (SDL) is however debated and no evidence of a separate phase close to the CIGS/CdS interface has been found [10,12,13]. It has been shown by modelling that an internal valence band offset (VBO) close to the interface is beneficial to the cell efficiency [7]. Modelling of CIGS solar cell has been performed frequently both with (e.g. Refs. [14–17]) and without SDL (e.g. Refs. [18,19]). In this work both modelling with and without SDL is done.

The established baseline set of parameters can function as a good starting point for modelling CIGS solar cells having different compositions and electrical properties. The strategy when modelling the cells is to measure as many properties as possible of the different cell structures and to change as few parameters as possible in SCAPS between the different structures. In previous work lightsoaking measurements on CIGS solar cells with atomic layer deposited (ALD) $Zn_{1-x}Mg_xO$ buffer layers were performed and a metastable increase in the fill factor (FF) under white light illumination was found [20]. This effect was stronger for cells with higher Mg-content. From four-point probe and Hall effect measurements on ALD-$Zn_{1-x}Mg_xO$ films of varying thickness and composition it was found that these exhibit light-induced persistent photoconductivity (PPC) [21]. All films were found to be of n-type conductivity and free carrier concentration and mobility in the relaxed as well as in the lightsoaked state were determined. PPC was more pronounced for thinner Mg-rich films. Here initial modelling of cells with ALD-$Zn_{1-x}Mg_xO$ buffer layers is carried out in SCAPS by utilising Hall measurement data. This is done with the aim to see if the FF improvement during illumination can be attributed to PPC in the buffer layer.

2. Setting the baseline

2.1. Selection of modelling parameters

All SCAPS simulations in this work have been performed under an AM 1.5 light spectrum. Series resistance, fitted from measured JV-curves, is included in the simulations. The baseline set of parameters for electrical modelling was obtained from measurements done in the group, measurement data found in literature and previous work by others dealing with modelling of CIGS solar cells. This parameter set is presented in Tables 1 and 2.

Many parameters are largely unknown and therefore have to be guessed by fitting the JV and QE-simulation results to measurement data. For modelling the absorber layers the recently added grading feature presented in Ref. [22] in SCAPS was utilised. Details about the modelled CIGS solar cells are found in Ref. [20]. The absorber layers

* Corresponding author. Tel.: +46 18 4713113; fax: +46 18 555095.
E-mail address: jonas.pettersson@angstrom.uu.se (J. Pettersson).

0040-6090/$ – see front matter
doi:10.1016/j.tsf.2010.12.141

Table 1
Baseline parameters for modelling CIGS cells with CdS buffer layer. In the table (a) and (d) denote shallow acceptor and donor defects while (A),(D) and (N) denote deep acceptor, donor and neutral defects.

Layer properties					
	CIGS	SDL	CdS	Undoped ZnO	Doped ZnO
Thickness [μm]	1.8	0.015	0.05	0.1	0.3
E_g [eV]	Graded	1.3	2.4	3.3	3.3
ϵ_r	13.6	13.6	5.4	9	9
N_C [cm^{-3}]	$6.8*10^{17}$	$6.8*10^{17}$	$1.3*10^{18}$	$3.0*10^{18}$	$3.0*10^{18}$
N_V [cm^{-3}]	$1.5*10^{19}$	$1.5*10^{19}$	$9.1*10^{18}$	$1.7*10^{19}$	$1.7*10^{19}$
v_{th}^e [cm/s]	$3.9*10^7$	$3.9*10^7$	$3.1*10^7$	$2.4*10^7$	$2.4*10^7$
v_{th}^p [cm/s]	$1.4*10^7$	$1.4*10^7$	$1.6*10^7$	$1.3*10^7$	$1.3*10^7$
μ_e [cm^2/Vs]	100	10	72	100	100
μ_p [cm^2/Vs]	12.5	1.25	20	31	31
Doping [cm^{-3}]	10^{16} (a)	10^{16} (a)	$5*10^{17}$ (d)	10^{17} (d)	10^{20} (d)
Bulk defect properties					
N [cm^{-3}]	10^{14} (D)	10^{14} (D)	$5*10^{16}$ (A)	10^{16} (A)	10^{16} (A)
σ_e [cm^2]	10^{-13}	10^{-13}	10^{-15}	10^{-15}	10^{-15}
σ_p [cm^2]	10^{-15}	10^{-15}	$5*10^{-13}$	$5*10^{-13}$	$5*10^{-13}$

Interface properties			
	CIGS/SDL	SDL/CdS	CdS/undoped ZnO
CBO [eV]	0.0	0.0	−0.2
N [cm^{-2}]	10^{11} (N)	$3*10^{13}$ (N)	–
σ_e [cm^2]	10^{-15}	10^{-15}	–
σ_p [cm^2]	10^{-15}	10^{-15}	–

were deposited in a system that produces layers of graded composition with regards to the group III elements [1]. This can be described with the compositional ratio defined in Eq. (1).

$$GGI = \frac{[Ga]}{[Ga] + [In]} \tag{1}$$

A grading profile was obtained from SIMS data while the mean GGI of 0.41 was measured with X-ray fluorescence. The grading profile was approximated with a straight line in SCAPS. In simulations the band gap and the electrical affinity were set to vary with composition. The dependence of the band gap on GGI was implemented using Eq. (2) [23,24].

$$E_g = 1.01 + 0.626 * GGI - 0.167 * GGI * (1 - GGI) \tag{2}$$

This gives a band gap variation between 1.34 eV at the back contact and 1.08 eV at the front surface. Almost all of the band gap widening is due to a change in the energetic position of the conduction band minimum [25]. In addition to the band gap also the absorption coefficients of CIGS are set to vary with composition based on the optical constants found in Refs. [26,27]. Optical constants of CBD CdS were drawn from the same work while absorption coefficients of the undoped and Al-doped ZnO layers were obtained from reflection–transmission (RT) measurements presented in Ref. [28]. A hole carrier concentration of about $10^{16}cm^{-3}$ is often found in CIGS layers [29,30]. Values on the effective electron and hole masses of the layers are drawn from literature [31–33]. Density of states at the conduction band minimum (N_c) and valence band maximum (N_v) are calculated using Eq. (3) (Ref. [32])

$$N_{c/v} = 2\left(\frac{2\pi m_{e/p}^* kT}{h^2}\right)^{3/2} \tag{3}$$

where $m_{e/p}^*$ are the effective band masses of electrons/holes, h is Planck's constant and k is the Boltzmann constant. Thermal velocities for electrons (v_{th}^e) and holes (v_{th}^p) are obtained from Eq. (4) [32].

$$v_{th}^{e/p} = \sqrt{\frac{3kT}{m_{e/p}^*}} \tag{4}$$

Mobilities are chosen in such a way that the following approximate relation holds [32].

$$\frac{\mu_p}{\mu_e} \approx \frac{m_e^*}{m_p^*} \tag{5}$$

In the CIGS the mobility is chosen so that the electron diffusion length has a reasonable value of about 0.8 μm [34]. Following the results in Ref. [9] no conduction band offset (CBO) was introduced between the CIGS and CdS layers. All layers are polycrystalline and therefore contain a large number of different defects which may be process dependent. This is especially true for the CIGS layer [35]. To keep the model as simple as possible, one type of single level defects are introduced in each layer. These are all compensating defects positioned at the intrinsic level that is close to midgap. Neutral interface defects for recombination were also positioned at midgap. Neutral crossections were selected in the range 10^{-18} – 10^{-15} cm^2 while attractive ones were selected in the range 10^{-13} – 10^{-12} cm^2 following Refs. [18,36]. To pin the Fermi level at the absorber/CdS interface, donor defects were placed 0.2 eV below the conduction band with the properties shown in Table 2. These have small capture crossections to separate between pinning and recombination. Parameters of the SDL are similar to the bulk CIGS except for the VBO and a higher mobility. Ohmic contacts are chosen. Experimental optical reflection data for finished solar cell stacks was utilised as a reflection filter in SCAPS. This filter was adjusted at long wavelengths to take into account the optical loss due to free carrier absorption in the highly doped ZnO.

Table 2
Parameters of defect used for Fermi level pinning at SDL/CdS interface. In the table (D) denotes deep donor defects.

Defect for pinning at SDL/CdS interface	
N [cm^{-2}]	$3*10^{13}$ (D)
σ_e [cm^2]	10^{-18}
σ_p [cm^2]	10^{-18}

2.2. Results

In Fig. 1 JV and QE results from simulations with the baseline parameters, including an SDL and with the Fermi level pinned, are compared with measurement data. All measurements were

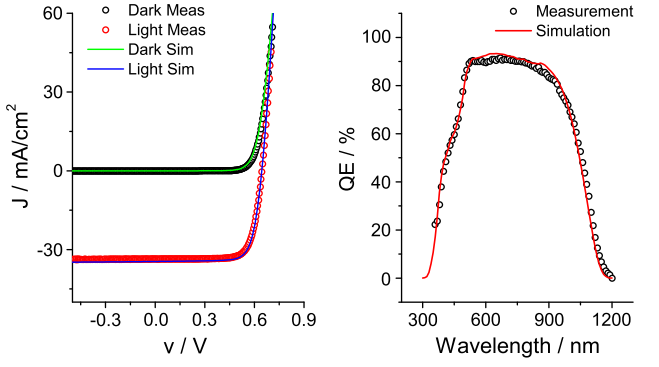

Fig. 1. Results from modelling with baseline parameters including an SDL compared with measured curves. The Fermi level is pinned by donor defects at the SDL/CdS interface. On the left hand side JV-curves obtained in light and in darkness are shown while to the right QE-curves are displayed.